Supporting Information

Highly-ordered supportless 3-D nanowire networks with tunable complexity and interwire connectivity for device integration

Markus Rauber[†,‡,], Ina Alber[‡], Sven Müller[‡], Reinhard Neumann[‡], Oliver Picht[‡], Christina Roth[†], Alexander Schökel[†], Maria Eugenia Toimil-Molares[‡], and Wolfgang Ensinger[†]*

[†] Department of Material- and Geo-Sciences, Technische Universität Darmstadt, Darmstadt, Germany

[‡] Materials Research Department, GSI Helmholtzzentrum für Schwerionenforschung GmbH, Darmstadt, Germany

[*] Author e-mail address: m.rauber@gsi.de

Contents

1. Experimental details

Chemicals
Dichloromethane (L-S Labor Service, CH_2Cl_2, 99.5%), ethanol (Carl Roth, EtOH, 99.5%), sodium hydroxide (L-S Labor Service, 97%), potassium iodide (L-S Labor Service, KI, 99.5%), and iodine (Merck, I_2, 99.999%) were used as received.

1.1 Nanowire network production

Template fabrication
Polycarbonate membranes with a thickness of 10-100 µm were irradiated in several steps at the linear accelerator *UNILAC* at GSI Darmstadt with Au and U ions of a kinetic energy of 11.1 MeV/u, applying total fluences of $1.4 \times 10^9 - 3 \times 10^{10}$ ions/cm². According to the desired branching geometries, the templates were irradiated various times from different directions.
In a typical irradiation experiment, the polymer membrane was first irradiated at an incident angle of 45° with respect to the surface. After the first irradiation step, the membrane was turned in plane by 90° and irradiated again at an incident angle of 45°. This procedure was repeated twice again until the membrane was irradiated 4 times from 4 different directions. For more complex network structures the total number of irradiation steps was increased.
Chemical etching in aqueous 6 M NaOH solution at 50°C led to the formation of a network of nanochannels with cylindrical geometry. The diameter is a function of the etching time as reported for nanowire arrays.[1, 2]

Electrochemical deposition
Prior to electrodeposition of nanowire networks (NWNs), a thin Au layer was sputter-deposited on one side of the template and reinforced electrochemically by Cu serving subsequently as a cathode. Electrochemical deposition into the nanochannel network templates was performed from an alkaline platinum bath (Platinum-OH, Metakem) at 60°C applying a cathodic potential of U = -1.3 V and, respectively, an Au electrolyte (Au-SF, Metakem) at 50°C applying a potential of U = -1 V in a two-electrode cell.
During the deposition current-time curves were recorded. Assuming an efficiency of the deposition reaction of 100%, the total mass of a network can be calculated from the employed charge Q by the Faraday law:

$$m = \frac{M \cdot Q}{z \cdot F}$$
(1)

with $\quad m$ = total mass of the deposited material
$\qquad M$ = molar mass of the deposited material
$\qquad Q$ = electric charge employed during deposition
$\qquad z$ = ion charge state
$\qquad F$ = Faraday constant

The mass of the networks, determined by equation 1, is in excellent agreement with the mass quantified by using a microbalance (AT20, Mettler Toledo).

According to requirements, the Cu and Au layers, which served as cathode, were removed after electrodeposition by nitric acid and an aqueous solution of KI and I_2, respectively. The polymer template was dissolved in dichloromethane for nanowire network characterization. The obtained networks could be purified by exchanging the solvent repeatedly and washing with ethanol. In addition, to remove all polymer residues and other impurities, the nanostructures were treated with 1 M NaOH at 50°C for 30 minutes and washed several times with deionized water. This cleaning procedure is important for subsequent characterization methods, especially surface area measurements.

Segmented Pt and multilayered Co/Pt nanowire networks were fabricated adopting methods that were used to grow nanowire arrays as described elsewhere.[3, 4]

1.2 Structural characterization

Electron microscopy, energy dispersive X-ray spectroscopy and X-ray diffraction

Field-emission scanning electron microscopy (FESEM) was employed to investigate the structure and branching geometries of the nanowire networks using a JSM-7401 microscope (JEOL) operated at 10-30 kV. The microscope was equipped with a detector (XFlash 5030, Bruker) for energy dispersive X-ray spectroscopy (EDX) allowing the determination of the composition of the samples. In addition, a detector (JEOL) measuring the transmission was used to perform scanning transmission electron microscopy (STEM).

To analyze network nodes in detail and crystallites of the nanowires, transmission electron microscopy (TEM, 4000FX, JEOL, 400 kV) was employed. Pt nanoparticles and in polymer embedded nanowire networks were studied by X-ray diffraction (XRD) in order to obtain information about the crystallite orientation using a HZG-4 goniometer in a Bragg-Brentano geometry and a Seifert X-ray generator providing Cu K_α radiation.

1.3 Electrochemical experiments

Electrode preparation

As working electrodes Pt nanowire networks were used on simple Au wire electrodes and commercial Pt catalysts on glassy carbon electrodes including platinum black (PtB, 28.1 m^2/g, Alfa Aesar) and platinum nanoparticles on a high surface area carbon support (Pt/C, 20 wt. % Pt HiSPEC 3000, Alfa Aesar). Figure S1 illustrates the preparation method of the glassy carbon catalyst electrodes, which was adopted and modified from previous reports.[5-8] In brief, aqueous suspensions containing 5 $mg_{catalyst}$/ml for PtB and 2 $mg_{catalyst}$/ml for Pt/C were produced by ultrasonic mixing for 20 minutes to obtain the catalyst ink. Before serving as a support for the catalysts, glassy carbon electrodes (GCE, 0.25 cm^2, SPI Supplies) were cleaned and polished. A defined volume of catalyst ink was pipetted onto the GCE, leading to loadings of 0.1 – 1 mg Pt/cm^2 for PtB and 0.1 – 0.6 mg Pt/cm^2 for Pt/C. After drying in air to eliminate solvent, the catalyst layer was covered with 20 μl of a 0.125% Nafion solution diluted from an initial 5 wt %

Nafion stock solution (Sigma-Aldrich). Subsequently, the electrodes were dried in an oven at 80°C for about 30 minutes.

Cyclic voltammetry studies

The cyclic voltammetry (CV) studies were performed in a conventional three-electrode cell at room temperature using a Reference 600 potentiostat (Gamry Instruments). A platinized titanium mesh was employed as counter electrode. All potentials were measured with a $Hg/HgSO_4$ reference electrode, but are given with respect to the reversible hydrogen electrode (RHE) in this paper.

For the determination of the electrochemical active surface area (ECSA) the potential was cycled between 0 and 1.3 V versus RHE in nitrogen purged 0.5 M H_2SO_4 solution with a scan rate of 50 mV/s. The area of hydrogen adsorption/desorption between 0 – 0.4 V has been frequently used to estimate the ECSA of Pt-based catalysts.[7-9] In this study, the charge for hydrogen desorption $Q_{H,d}$ was used to calculate the ECSA by means of equation 2:

$$ECSA = \frac{Q_{H,d}}{m \times c} \tag{2}$$

with $\quad Q_{H,d}$ = charge for hydrogen desorption (mC/cm^2)

$\quad\quad m \quad$ = Pt loading (mg/cm^2)

$\quad\quad c \quad$ = charge required to oxidize a monolayer of hydrogen (0.210 mC/cm^2 on Pt)

The ECSA standard deviation was calculated by equation 3:

$$\Delta ECSA = \left|\frac{\Delta Q_{H,d}}{[Pt] \times 0.21}\right| + \left|\frac{\Delta[Pt]Q_{H,d}}{[Pt]^2 \times 0.21}\right| \tag{3}$$

In the methanol oxidation reaction studies, CV curves were recorded between 0 and 1.3 V versus RHE in a nitrogen purged solution containing 0.5 M CH_3OH and 0.5 M H_2SO_4. The scan rate was 50 mV/s.
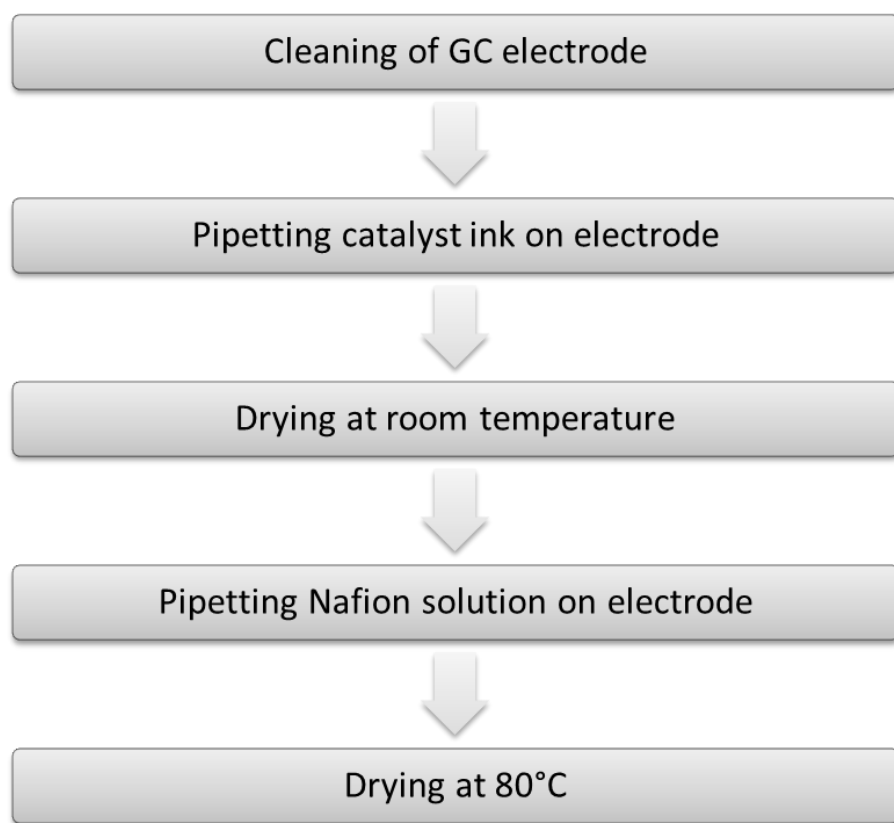
Figure S1: Schematic illustration of GC catalyst electrode preparation procedure.

2. Supporting data

2.1 Diameter distribution

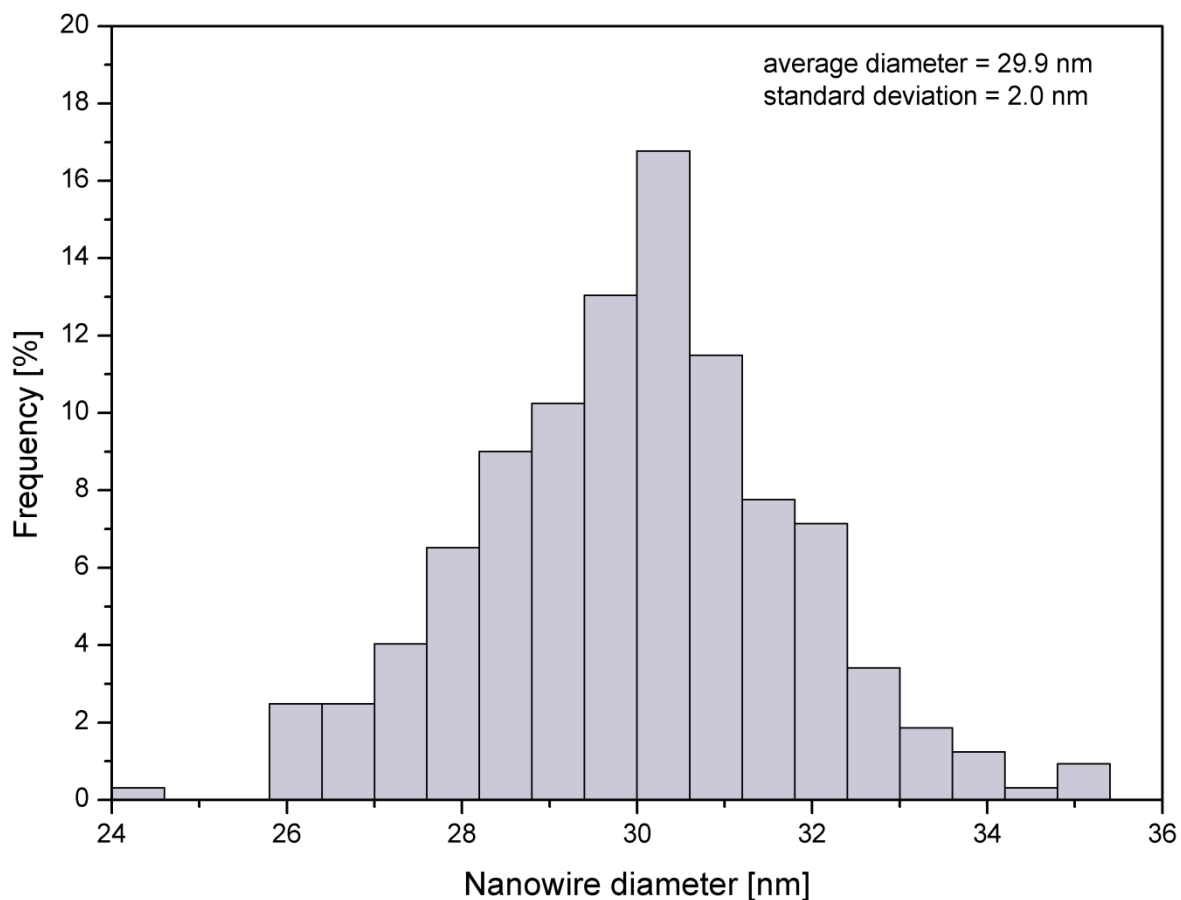average diameter = 29.9 nm
standard deviation = 2.0 nm

Figure S2: Histogram illustrating the diameter distribution for Pt nanowires in a nanowire network. More than 300 randomly selected wires at different areas of the network were investigated by scanning electron microscopy. The percentage ratio of the standard deviation to the average size is 6.7%. Absolute values are given in the graph.
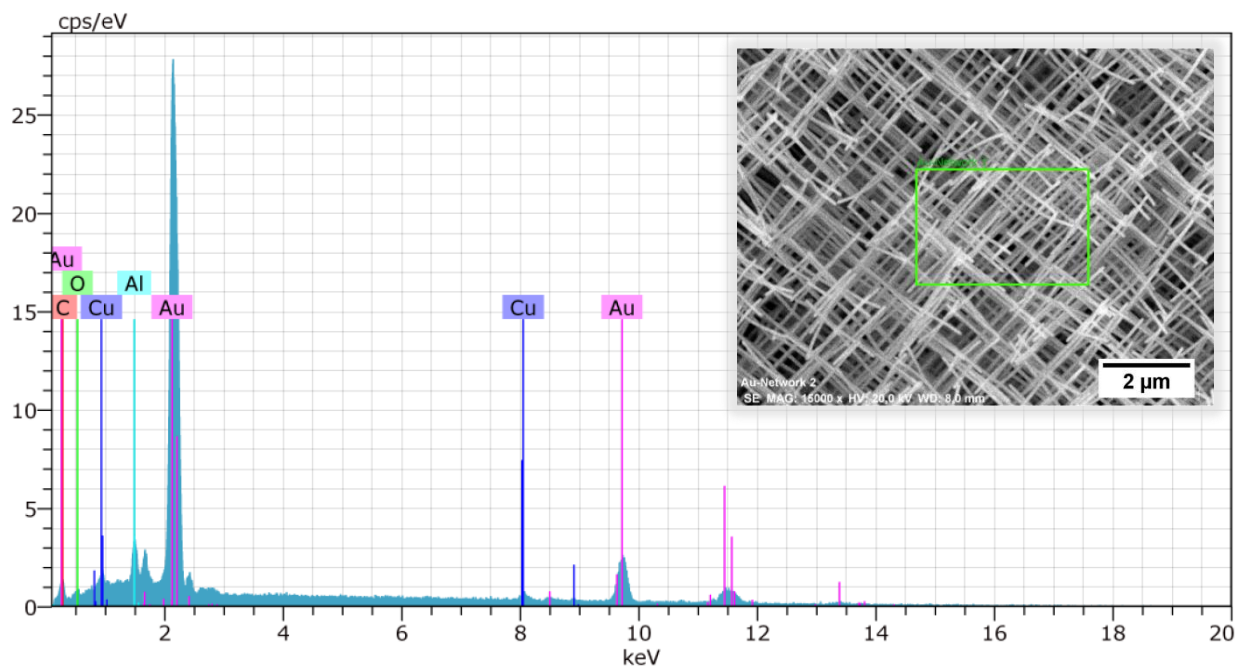
2.2 EDX analysis of Au, Pt, and CdTe NWNs

Figure S3: EDX analysis of an Au nanowire network. Cu and Al signals originate from the sample holder. The inset shows a SEM image of the associated NWN with sketched in investigated area.
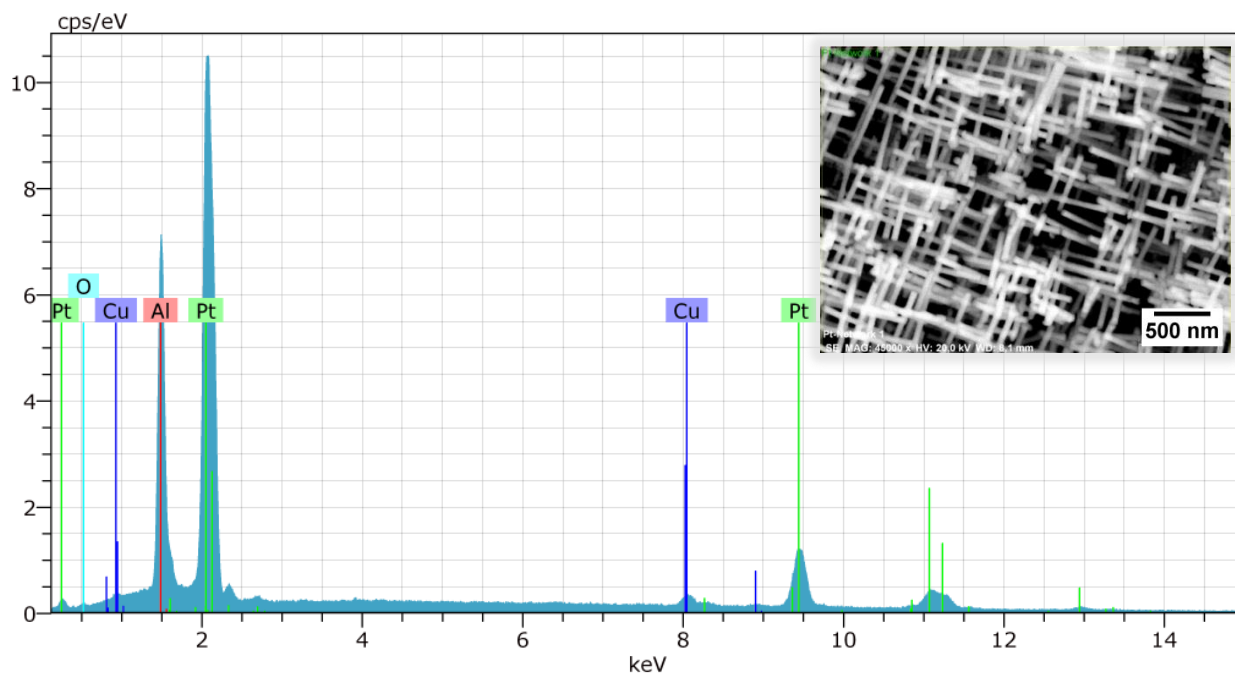

Figure S4: EDX analysis of a Pt nanowire network. Cu and Al signals originate from the sample holder. The inset shows a SEM image of the investigated area of the NWN.
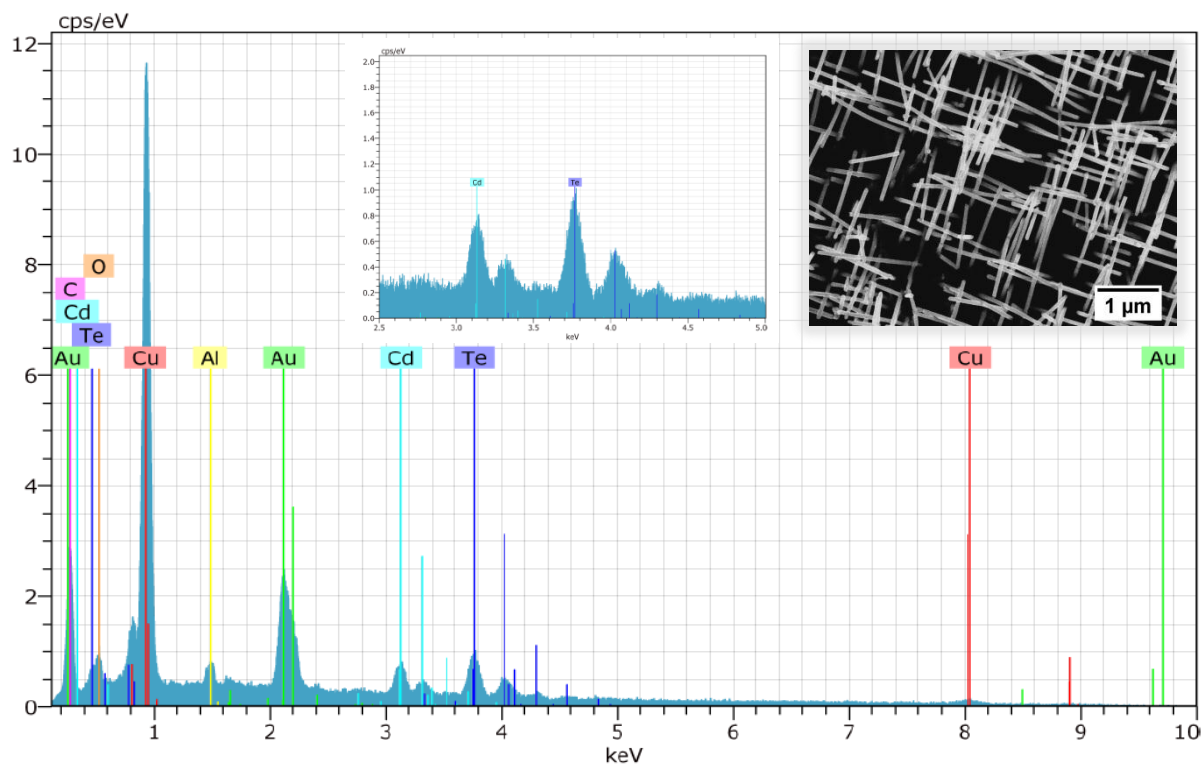
Figure S5: EDX analysis of a CdTe nanowire network. Cu and Au signals originate from the cathode layer, the Al signals from the sample holder. The insets show the Cd and Te signals (left) and a representative image of the investigated network area (right). The CdTe network was produced adopting a electrodeposition protocol from a work by T. Ohgai et al. reporting the synthesis of CdTe semiconductor nanowire arrays.[10]

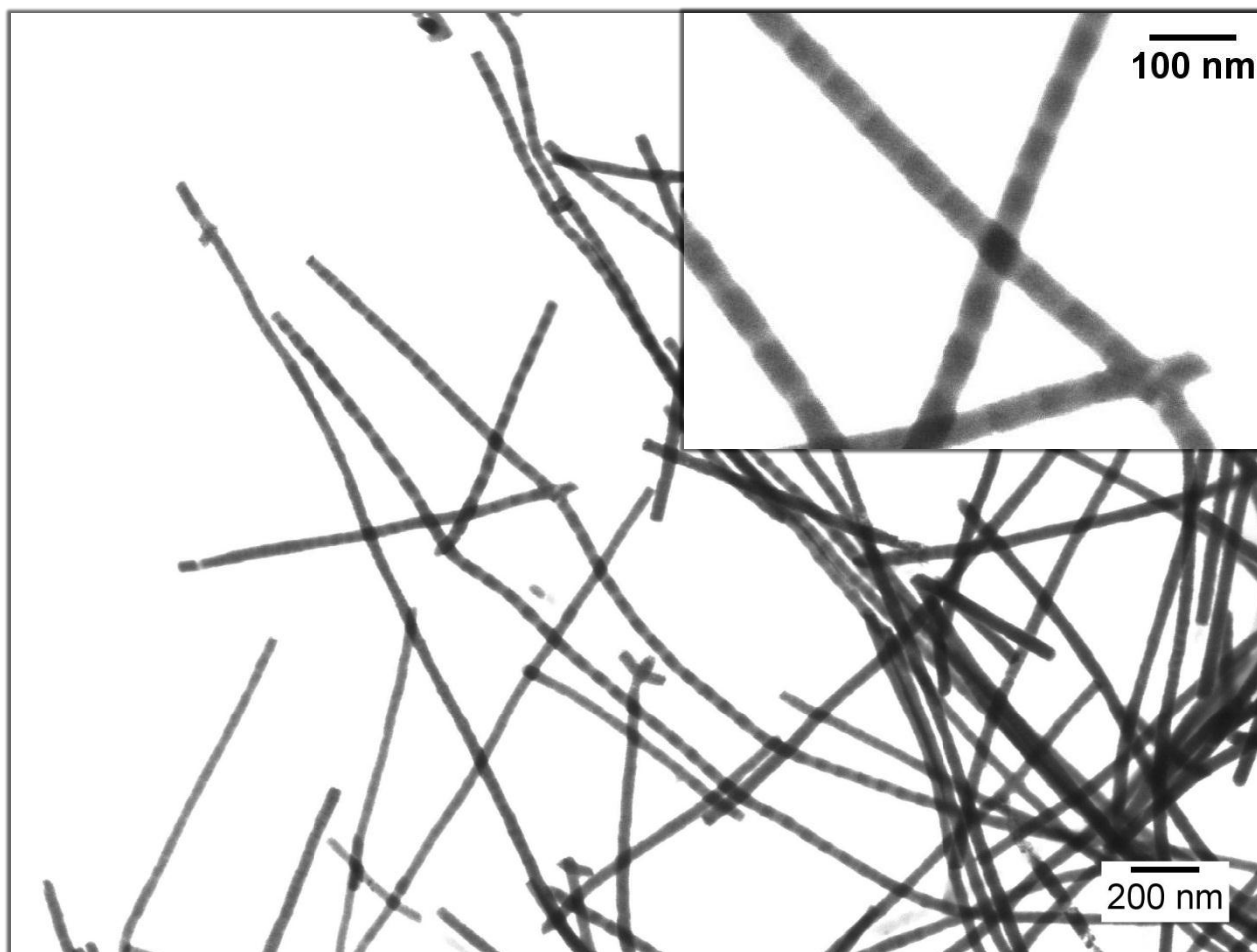**2.3 STEM characterization of Co/Pt NWNs**

Figure S6: STEM image of a nanowire network consisting of multilayered Co/Pt nanowires. The picture was taken at a thin edge of the network. Interconnected nanowires are depicted at higher magnification in the inset.

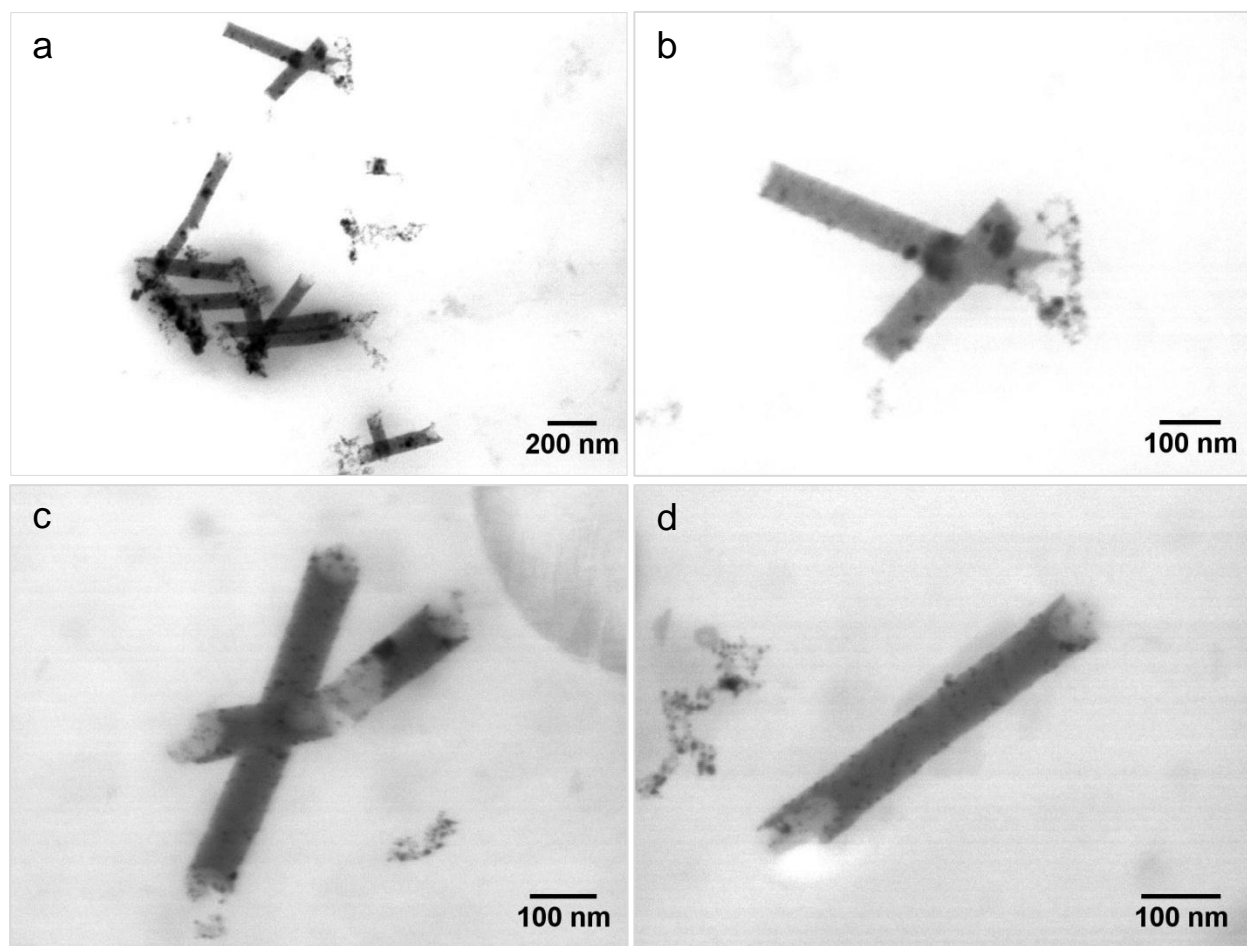**2.4 STEM characterization of nanotube networks**

Figure S7: STEM images of pieces of a nanotube network fabricated by an electroless two-step deposition process. The nanotubes form a stable network only while they are embedded in the template material. a-c) After dissolution of the polymer matrix, tube fragments show branching points that clearly indicate the initial creation of a nanotube network. d) The depicted piece shows a well-defined tube geometry with homogeneous wall thickness.
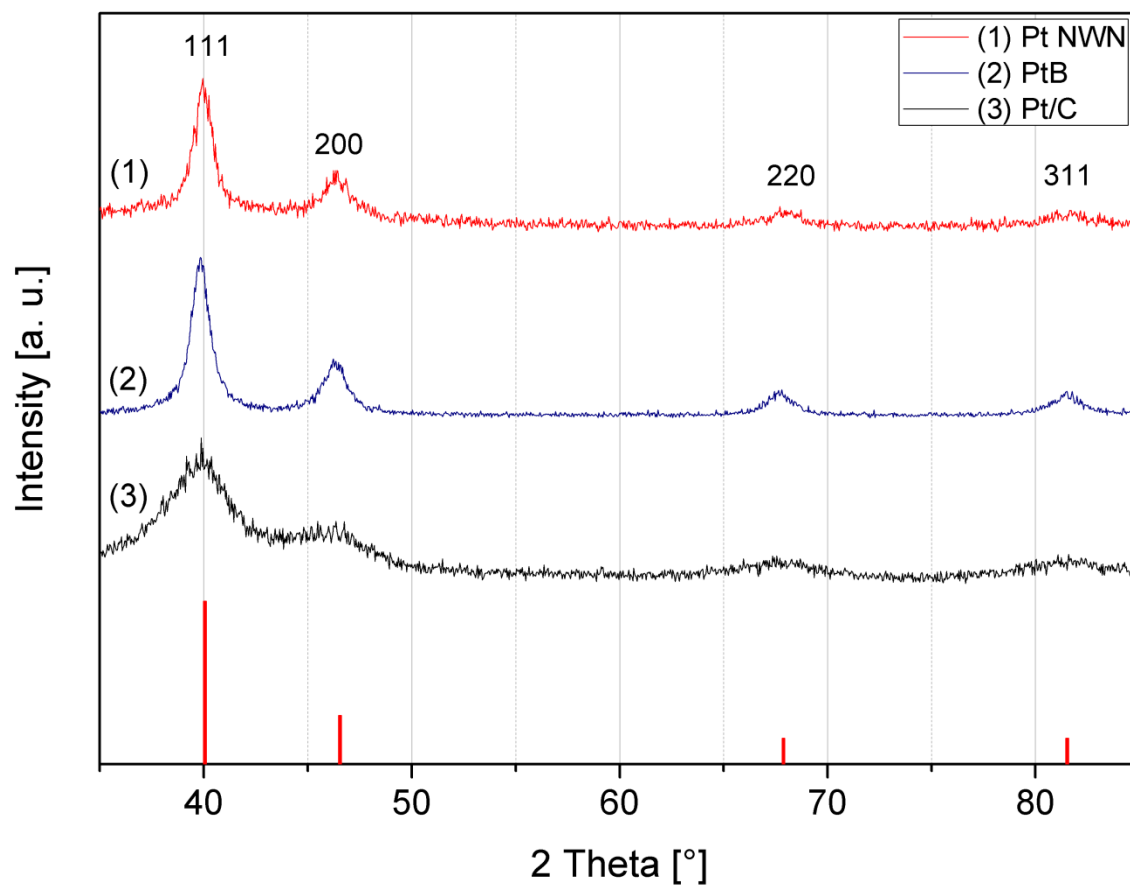
2.5 X-ray diffraction

Figure S8: XRD patterns of Pt NWNs, PtB, and Pt/C. Vertical lines represent the intensity distribution of a Pt powder sample.

3. References

1.   Kline, T. R.; Tian, M.; Wang, J.; Sen, A.; Chan, M. W. H.; Mallouk, T. E. *Inorg. Chem.* **2006,** *45*, 7555-7565.
2.   Ensinger, W.; Vater, P. *Mater. Sci. Eng., C* **2005,** *25*, 609-613.
3.   Rauber, M.; Brötz, J.; Duan, J.; Liu, J.; Müller, S.; Neumann, R.; Picht, O.; Toimil-Molares, M. E.; Ensinger, W. *J. Phys. Chem. C* **2010,** *114*, 22502-22507.
4.   Choi, J. R.; Oh, S. J.; Ju, H.; Cheon, J. *Nano Lett.* **2005,** *5*, 2179-2183.
5.   Koenigsmann, C.; Zhou, W.; Adzic, R.; Sutter, E.; Wong, S. *Nano Lett.* **2010**, *10*, 2806-2811.
6.   Song, Y.; Garcia, R. M.; Dorin, R. M.; Wang, H. R.; Qiu, Y.; Coker, E. N.; Steen, W. A.; Miller, J. E.; Shelnutt, J. A. *Nano Lett.* **2007,** *7*, 3650-3655.
7.   Chen, Z. W.; Waje, M.; Li, W. Z.; Yan, Y. S. *Angew. Chem. Int. Ed.* **2007,** *46*, 4060-4063.
8.   Pozio, A.; De Francesco, M.; Cemmi, A.; Cardellini, F.; Giorgi, L. *J. Power Sources* **2002,** *105*, 13-19.
9.   Choi, S. M.; Kim, J. H.; Jung, J. Y.; Yoon, E. Y.; Kim, W. B. *Electrochim. Acta* **2008,** *53*, 5804-5811.
10.   Ohgai, T.; Gravier, L.; Hoffer, X.; Ansermet, J. P. *J. Appl. Electrochem.* **2005,** *53,* 479-485.